

Population of isomers in the decay of the giant dipole resonance

N. Tsoneva and Ch. Stoyanov

Institute for Nuclear Research and Nuclear Energy, 1784 Sofia, Bulgaria

Yu. P. Gangrsky and V. Yu. Ponomarev*

Joint Institute for Nuclear Research, 141980, Moscow region, Dubna, Russia

N. P. Balabanov

P. Khilendarsky University, Plovdiv, Bulgaria

A. P. Tonchev

Department of Physics, Idaho State University, Pocatello, Idaho 83209

(Received 16 September 1999; published 24 February 2000)

The value of an isomeric ratio (IR) in $N=81$ isotones (^{137}Ba , ^{139}Ce , ^{141}Nd , and ^{143}Sm) is studied by means of the (γ, n) reaction. This quantity measures a probability to populate the isomeric state in respect to the ground state population. In (γ, n) reactions, the giant dipole resonance (GDR) is excited and after its decay by a neutron emission, the nucleus has an excitation energy of a few MeV. The forthcoming γ decay by direct or cascade transitions deexcites the nucleus into an isomeric or ground state. It has been observed experimentally that the IR for ^{137}Ba and ^{139}Ce equals about 0.13 while in two heavier isotones it is even less than half the size. To explain this effect, the structure of the excited states in the energy region up to 6.5 MeV has been calculated within the quasiparticle phonon model. Many states are found connected to the ground and isomeric states by $E1$, $E2$, and $M1$ transitions. The single-particle component of the wave function is responsible for the large values of the transitions. The calculated value of the isomeric ratio is in very good agreement with the experimental data for all isotones. A slightly different value of maximum energy with which the nuclei rest after neutron decay of the GDR is responsible for the reported effect of the A dependence of the IR.

PACS number(s): 23.20.-g, 21.60.-n, 27.60.+j

I. INTRODUCTION

Considerable interest in the structure of the states at intermediate excitation energy in atomic nuclei has arisen recently [1–10]. The states are excited via different nuclear reactions and the deexcitation populates the low-lying excited states that have a simple structure [1]. The study of the electromagnetic transitions coupling low-lying states with those having intermediate energy reveals a delicate interplay between the main excitation modes in atomic nuclei—single-particle and the collective ones [6].

Isomers have been known for more than 50 years and during this period very precise spectroscopic information about their properties has been obtained (see, e.g., the review article [1]). They have relatively low excitation energy and total angular momentum J_{iso} , which is very different than the angular momentum of the ground state, $J_{\text{g.s.}}$. Due to these specific properties, their electromagnetic decay into the ground state is strongly hindered and they are characterized by a half-life from ms to years depending on the value of $|J_{\text{iso}} - J_{\text{g.s.}}|$. The nuclear isomer population is studied by means of (γ, γ') , (n, γ) , (γ, n) , $(n, 2n)$ reactions and β decay. The different nuclear reactions show the contribution of the single-particle and the more complex components in the structure of their wave function.

Recently, essential progress in isomer photoexcitation has been achieved by using bremsstrahlung radiation at low values of an end-point energy [6–9]. The isomer yield in spherical nuclei as a function of the end-point energy was found to have a linear dependence in the energy interval of about one MeV, the line then breaks, and another linear dependence for one MeV takes place. This effect received its theoretical interpretation as follows: A level or a group of closely lying levels with very specific properties are located at the line break. The wave function of these excited states includes configurations which allow their intensive excitation from the ground state while some other configurations are responsible for a cascade decay from these levels at intermediate energies which lead to the isomeric state [6–9]. Usually the maximum value of the end-point energy in these bremsstrahlung experiments is 4–4.5 MeV.

An alternative way to populate the isomeric states is offered by the (γ, n) reaction, applying the end-point energy of the bremsstrahlung radiation from 10 to 25 MeV. In this reaction the giant dipole resonance (GDR) is initially excited. The main mechanism of its decay in the heavy nuclei is related to the neutron emission. The nucleus rests with the excitation energy of 5–7 MeV and decays by γ transitions into the isomeric and ground states. Since the excitation energy of intermediate states reached in this reaction is relatively high, the statistical approach is usually used for a theoretical interpretation of the γ decay process [11–13].

In the present paper we present the experimental results for the population of $h_{11/2}$ isomers in $N=81$ isotones in the

*Present address: Vakgroep Subatomaire en Stralingsfysica, Universiteit Gent, Proeftuinstraat 86, 9000 Gent, Belgium.

(γ, n) reaction. It will be reported that at $E_\gamma = 25$ MeV the isomeric ratio (IR) equals 0.12, 0.14, 0.06, and 0.046 in ^{137}Ba , ^{139}Ce , ^{141}Nd , and ^{143}Sm , respectively. All these nuclei have identical spins and parities in their isomeric and ground states. Therefore, the IR should not be affected by such factors as the difference between the spin of the isomeric ($J^\pi = 11/2^-$) and ground states ($J^\pi = 3/2^+$). Moreover, the isomeric levels for the isotopes ^{139}Ce , ^{141}Nd , and ^{143}Sm have an energy on the order of 755 and 661 keV in ^{137}Ba . It is clear that it is not possible to explain the difference between two lighter and two heavier nuclei by statistical properties of intermediate states without additional assumptions. It means that the structure of the excited states is important even at these excitation energies, and it should be accounted for. For this reason, a microscopic calculation should be applied to explain the A dependence of the isomer yield which is experimentally observed. For that purpose, we employ the quasiparticle phonon model (QPM) which has already been successfully applied to the interpretation of the isomer population from the intermediate states at lower energies [6–9].

The structure of the states at intermediate excitation energy is rather complex. The interplay of the simple collective and the more complex modes leads to the fragmentation of the simple excitations. The experimental data as well as theoretical calculations reveal the spreading of the simple modes in a wide energy region, where large fluctuations in strength are obtained. A convenient approach to describe the fragmentation is based on the doorway picture [14,15]. This approach incorporated in the QPM permits the description of different processes, where excited states with intermediate energy are included: γ decay [16], nucleon emission [17], etc.

The paper is organized as follows. In Sec. II some details of the (γ, n) experiment are discussed and the experimental results are presented. A theoretical treatment of the (γ, n) reaction is given in Sec. III. In Sec. III A we discuss the mechanism of the reaction while details of the nuclear structure calculations in odd mass nuclei within the QPM are given in Sec. III B. The results of numeric calculations are discussed in Sec. IV in comparison with the experimental data.

II. EXPERIMENTAL RESULTS

The measurements of the IR were performed on the electron accelerator microtron MT-25 of Flerov Laboratory of Nuclear Reactions, JINR. The description of this microtron and its main parameters were published earlier [1]. The essential advantage of this accelerator is the small energy spread of the accelerated electrons (30–40 keV) at the high beam intensity (up to an average power 600 W). This allows measurement of the cross sections of the studied nuclides production at the strictly definite end-point energy.

The electron beam extracted from the accelerator chamber was focused by using the quadrupole lenses and directing it on the stopping target, which consists of a 2 mm thick tungsten disk cooled by water. The electron spot on the target was about 5 mm. The mean current on the target $20 \mu\text{A}$ was

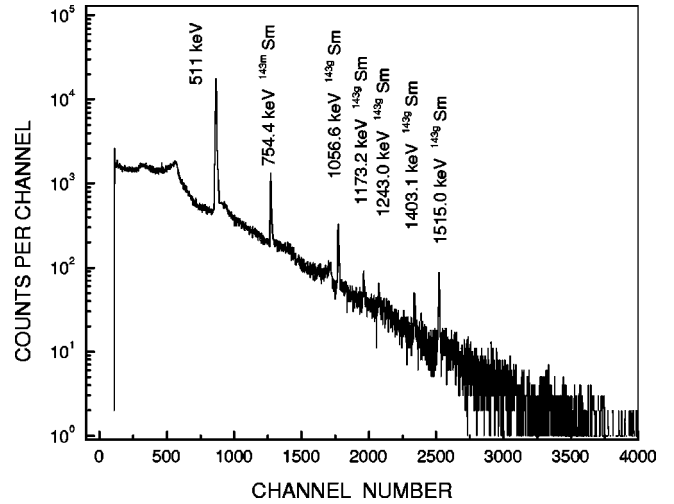


FIG. 1. γ -ray spectrum measured after activation of ^{144}Sm target by bremsstrahlung radiation with endpoint energy $E_{\gamma_{\max}} = 25$ MeV. The γ -lines used in the data analysis are indicated for the isomeric and ground states.

measured continuously during the experiment. The energy of the electron beam (and the upper boundary of the bremsstrahlung) was changed by two methods: the choice of the proper electron orbit and the tuning of the magnetic field.

The oxides of the studied elements, BaO , Ce_2O_3 , Nd_2O_3 , and Sm_2O_3 , were irradiated by the bremsstrahlung spectrum. They have a weight of ~ 100 mg, a surface area $\sim 1 \text{ cm}^2$, and were enriched by the studied isotope up to 93%. The irradiation time was 10 min for each target. The irradiation flux was monitored by Cu activation foils that were irradiated simultaneously with the samples. About one min after the end of irradiation, the residual activity from the isotones samples and Cu monitor, were measured separately by a calibrated 60 cm^3 Ge(Li) detector with an energy resolution of $\Delta E = 2.5 \text{ keV}$ for $E_\gamma = 1332 \text{ keV}$ of ^{60}Co . The detector was operated in a lead shielding chamber lined with a 10 cm thick wall. Measurements have been repeated to determine experimentally the half-life of the radioactive nuclides under study. The spectra were processed according to the ACTIV code, which permits separating γ lines with close energies in the complicated spectrum. Figure 1 shows one of the measured γ spectrum obtained upon irradiating an enriched ^{144}Sm isotope by bremsstrahlung with an end point energy of 25 MeV. The γ lines corresponding to β - γ decay of unstable ^{143}Sm in the ground and the isomeric states into ^{143}Pm are clearly seen in the spectrum.

The IR is determined by the ratio of the measured nuclei yields in the isomeric and the ground state,

$$\text{IR} = \frac{Y(E_{\gamma_{\max}})_m}{Y(E_{\gamma_{\max}})_g}, \quad (1)$$

where the indices m and g are attributed to the isomeric and ground states, respectively; Y is the yield of isomeric or ground state, and $E_{\gamma_{\max}}$ is the maximum endpoint energy. The ratio of the yield is connected with the areas under the γ

peaks corresponding to the isomeric and ground states (S_m and S_g , respectively) by the equation

$$\frac{Y(E_{\gamma_{\max}})_m}{Y(E_{\gamma_{\max}})_g} = \left[\frac{\lambda_g f_m(t)}{\lambda_m f_g(t)} \left(\frac{S_g \epsilon_m I_m (1 + \alpha_g)}{S_m \epsilon_g I_g (1 + \alpha_m)} - p \frac{\lambda_g}{\lambda_g - \lambda_m} \right) + p \frac{\lambda_m}{\lambda_g - \lambda_m} \right]^{-1}, \quad (2)$$

where α is a conversion coefficient of γ radiation, I is the probability of the γ -ray emission, ϵ is the efficiency of the Ge(Li) detector for the corresponding γ line, λ is the decay constant, p is the probability of the transition from an isomeric to a ground state, and the time factor $f(t)$ that takes into account the accumulation and decay of the nuclei is given by

$$f(t_i, t_c, t_m) = (1 - e^{-\lambda_g t_i}) e^{-\lambda_g t_c} (1 - e^{-\lambda_g t_m}), \quad (3)$$

where t_i , t_c , and t_m are the times of irradiation, decay, and measurement. Because the isomeric and ground states were obtained in the same exposure run, and because the required quantities (yields or cross sections) were measured for them under identical conditions, the errors associated with the intensities of the bremsstrahlung flux and the geometry of exposures and measurements were eliminated in the determining IRs.

The nuclei produced in (γ, n) reactions are radioactive both in the ground and isomeric states (except ^{137}Ba). Therefore it was possible to determine the yields of studied nuclei in the ground and isomeric states simultaneously by measuring the intensity of the emitted γ -radiation using Eq. (2). For ^{137}Ba the IR determination by direct method becomes impossible for the lack of the appropriate γ lines in the ground state. Thus, the possibilities of isomer production of ^{137m}Ba isomer via (γ, n) reactions were investigated at energies $E_\gamma = 10$ –25 MeV. The yield of ^{137m}Ba was compared with the yield of monitoring reaction. The cross section for the reaction $^{63}\text{Cu}(\gamma, n)^{62}\text{Cu}$ measured in a beam of quasimonochromatic photons was taken as the reference from [18]. Reconstruction of reaction cross section, employing an iterative procedure, was depicted in our previous paper [2]. Figure 2 displays the cross section for (γ, n) reactions with production of the ^{137m}Ba isomeric state. In order to determine IR, the ^{137m}Ba cross section was subtracted from the total $^{137m+g}\text{Ba}$ cross section [18]. Thus, in the case of ^{137}Ba , the IR was defined as a cross section ratio. The values of these IR are in accordance with the previous results [2,3]. The IR dependence on the end-point energy is also given in Fig. 2. Three main regions of IR behavior are recognized. The first region is from the neutron threshold to a maximum in the photoabsorption cross section where the IR increases sharply. In the second region (from 16 to 21 MeV) of the high-energy tail of the GDR, the IR changes slightly. Above 21 MeV where the GDR tail becomes very weak, the IR turns out to be practically constant. Since the spin and parity of a compound nucleus does not change (it is always 1^- after dipole absorption), the observed increase in the IR is due to the enlargement of the interval of excitation energies

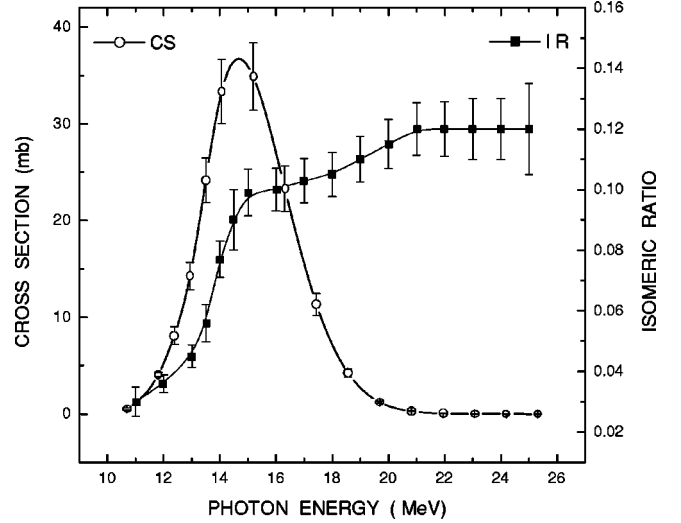


FIG. 2. Measured cross section for the reaction $^{138}\text{Ba}(\gamma, n)^{137m}\text{Ba}$ as a function of bremsstrahlung end-point energy. The isomeric ratio is plotted with the right-hand side axis.

of a residual nucleus in which photons that result in the population of the isomeric state occur.

The IR at $E_{\gamma_{\max}} = 25$ MeV are presented in the Table I. The values of these IR are in accordance with the previous results [2,4], but they are more precise. We have also added the IR for ^{141}Nd and ^{143}Sm from the β decay of ^{141}Pm and ^{143}Eu , respectively. They are obtained from the analysis of the decay schemes of ^{141}Pm and ^{143}Eu [19].

III. THEORETICAL TREATMENT OF THE ISOMER POPULATION IN (γ, n) REACTIONS

The process of the isomer population in (γ, n) reactions is rather complex and may be split into a few stages. In the first stage, the GDR is excited by bremsstrahlung radiation. In the second, it quickly decays into the compound nucleus. Next, the compound nucleus decays by emitting of neutrons, leaving the $(A - 1)$ nucleus with an excitation energy of a few MeV. In the last stage, the nucleus deexcites by direct or cascade γ transitions into the isomeric or ground state. Since

TABLE I. The calculated (QPM) isomeric ratio for (γ, n) reaction and β decay in comparison with the experimental results (Exp). E^* is the maximum energy of intermediate states reached in every reaction.

Reaction	E^* , MeV		Isomeric ratio	
	Exp	QPM	Exp	QPM
$^{138}\text{Ba}(\gamma, n)^{137m}\text{Ba}$	5.4	5.4	0.12(1)	0.10
$^{140}\text{Ce}(\gamma, n)^{139}\text{Ce}$	4.8	4.8	0.14(1)	0.11
$^{142}\text{Nd}(\gamma, n)^{141}\text{Nd}$	4.2	4.2	0.06(1)	0.05
$^{144}\text{Sm}(\gamma, n)^{143}\text{Sm}$	3.5	3.5	0.047	0.051
$^{143}\text{Eu} \xrightarrow{\beta} ^{143}\text{Sm}$	4.56	4.6	0.009	0.007
$^{141}\text{Pm} \xrightarrow{\beta} ^{141}\text{Nd}$	5.1	5.1	0.01	0.01

the width of γ decay strongly decreases with an increase of the multipolarity, the decays are mainly due to $E1$, $M1$, or $E2$ transitions. The excited states of the nucleus at intermediate energies, via which the isomers are populated, are called activated states (ASs). The specific properties of the ASs are the following: First, due to their total angular momentum and some components of their wave function, they tend to decay into the isomer than into the ground state. Secondly, the ASs should be excited themselves. The last depends on the nuclear reaction considered. For example, in bremsstrahlung experiments with the end-point energy of a few MeV, the AS state must have a total angular momentum not very different from those of the ground state in order to make their electromagnetic excitation with low multipolarity from the ground state possible. If (γ, n) reaction is applied, the ASs should have the total spin close to 1 since emitted neutrons in the GDR decay tend to take away a small angular momentum. Thus, in principle, different ASs may be involved in the population of isomers in the different nuclear reactions.

To some extent, the observed variations in the IR values can be associated with the distinctions between the excitation energy and the angular momentum distributions of the final nucleus prior to the photon direct or cascade decay populating the isomeric and ground state. In (γ, n) reactions, the excitation energy and the angular momentum distributions are determined by neutron emission from an excited nucleus produced as the result of photon absorption. The angular momentum distribution for the reaction (γ, n) on Ba, Ce, Nd, and Sm isotopes are similar. In this process, the neutron it emits from the state of an initial nucleus with spin and parity 1^- (dipole absorption) is followed by the population of the residual nucleus state with a spin $3/2^+$ (ground state) or $11/2^-$ (isomeric state). When the isomer population is such that all the nuclei under study are characterized by equal spins at each steps of the reaction, the IR is determined by the excitation energy with which the nuclei rest after neutron decay. In the latter case, the energy distribution was comparatively broad due to the bremsstrahlung spectrum of the γ radiation. The width of this distribution is mainly defined by the photoabsorption Lorentzian curve which is very similar to the studied isotones. The mean value of the excitation energy distribution E^* equals

$$E^* = E_{\text{eff}} - B_n - \varepsilon_n, \quad (4)$$

where E_{eff} is the effective excitation energy, B_n is the neutron binding energy, and ε_n is the kinetic energy of the neutron escaping from the compound nucleus. A peculiarity of the photonuclear reaction with a bremsstrahlung radiation is related to the fact that the whole bremsstrahlung spectrum is involved in the process of photoexcitation. The energy centroid is determined by the ratio

$$E_{\text{eff}} = \frac{\int_{E_{\text{th}}}^{E_{\gamma_{\text{max}}}} E_{\gamma} \sigma(E_{\gamma}) N(E_{\gamma}, E_{\gamma_{\text{max}}}) dE_{\gamma}}{\int_{E_{\text{th}}}^{E_{\gamma_{\text{max}}}} \sigma(E_{\gamma}) N(E_{\gamma}, E_{\gamma_{\text{max}}}) dE_{\gamma}}, \quad (5)$$

TABLE II. The experimental values of $T_{lj}(\varepsilon)$ for different angular momentum l of the emitted neutron with the energy $\varepsilon = 1$ MeV.

	$l=0$	$l=1$	$l=2$	$l=3$
T	0.55	0.33	0.05	0.006

where E_{th} is a threshold energy, $\sigma(E_{\gamma})$ is the cross section for the absorption of a photon with energy E_{γ} by a nucleus, and $N(E_{\gamma}, E_{\gamma_{\text{max}}})$ is the number of photons with energy E_{γ} in the bremsstrahlung spectrum. The experimental kinetic energy spectra of the neutrons with a mean energy of 1 MeV were used. The maximum excitation energy of the residual nuclei after (γ, n) reaction is presented in Table I.

A. Reaction mechanism

The main features of the (γ, n) process are discussed in Ref. [20]. The cross section for (γ, n) reaction with a population of the isomeric (ground) state may be schematically written as

$$\sigma_{\text{iso(g.s.)}} = \sigma_0 P_n^{lj} \frac{\Gamma_{\text{iso(g.s.)}}}{\Gamma_{\text{tot}}}, \quad (6)$$

where σ_0 is the photoabsorption cross section which describes the GDR excitation with formation of a compound nucleus and Γ_{iso} , $\Gamma_{\text{g.s.}}$, and Γ_{tot} are γ widths for decay to isomeric, ground state, and total decay width, respectively.

A relative probability P_n^{lj} of emission of a neutron with spin j and angular momentum l is given by the relation

$$P_n^{lj} = \frac{\sigma_n^{lj}}{\sum_{l'j'} \sigma_n^{l'j'}}. \quad (7)$$

The quantity σ_n^{lj} is the cross section of the emission of a neutron with spin j and angular momentum l with formation of a nucleus with momentum J and projection M and is equal to

$$\sigma_n^{lj} = \frac{\pi}{k^2} \frac{(2j+1)}{2} T_{lj}(\varepsilon) |(jJ'; 0m | jJ'; JM)|^2, \quad (8)$$

where $(jJ'; 0m | jJ'; JM)$ is a Clebsch-Gordan coefficient, J' is the spin of the compound nucleus; neutron wave number is denoted by k , the quantities $T_{lj}(\varepsilon)$ are the neutron penetrations. The energy ε corresponds to the average energy of the evaporated neutron from the compound nucleus. The experimental values of the factors $T_{lj}(\varepsilon)$ at $\varepsilon = 1$ MeV are presented in Table II. At this energy, the neutron could carry an angular moment $l=0, 1, 2$, and 3 [3]. The probabilities for $l \geq 4$ are very small and may be excluded from the consideration. In the actual calculation the GDR energy centroid has been taken from Ref. [18] and its width has been neglected.

Combining Eqs. (6)–(8) [21], the ratio $\sigma_{\text{iso}}/\sigma_{\text{g.s.}}$ for the (γ, n) reaction reads

$$\frac{\sigma_{\text{iso}}}{\sigma_{\text{g.s.}}} = \frac{\sum_{J_1^\pi} (2J_1 + 1) T_{l_1 j_1}(\varepsilon) \sum_{\vartheta} (C_{J_1^\pi}^\vartheta)^2 \Gamma_{J_1^\pi \rightarrow \text{iso}}^\vartheta}{\sum_{J_2^\pi} (2J_2 + 1) T_{l_2 j_2}(\varepsilon) \sum_{\vartheta} (C_{J_2^\pi}^\vartheta)^2 \Gamma_{J_2^\pi \rightarrow \text{g.s.}}^\vartheta}, \quad (9)$$

where $j_{1(2)}$ and $l_{1(2)}$ are the moments of the emitted neutron from the compound nucleus, $j_{1(2)} = |l_{1(2)} \pm 1/2|$ and $J_{1(2)} = j_{1(2)} + 1$, the quantities $(C_J^\vartheta)^2$ are the spectroscopic factors for the ϑ state with momentum and parity J^π of the final nucleus; $\Gamma_{J^\pi \rightarrow \text{iso}}^\vartheta$ ($\Gamma_{J^\pi \rightarrow \text{g.s.}}^\vartheta$) are the partial widths for the γ decay of the state J^π to the isomeric (ground) state. The value of Γ_J^ϑ includes, in principle, the all unknown cascades which the intermediate state J^π undergoes.

The partial widths Γ are connected with the corresponding reduced transition probabilities [20]

$$\Gamma_{J^\pi \rightarrow I^\pi}(\lambda\lambda) \sim E^{2\lambda+1} B(\lambda\lambda; J^\pi \rightarrow I^\pi), \quad (10)$$

where $B(\lambda\lambda)$ are the reduced transition probabilities in $e^2 \text{fm}^{2\lambda}$ for the electric and in $\mu_N^2 \text{fm}^{2\lambda-2}$ for the magnetic transitions; the quantity E is the γ -quanta energy.

B. Structure of excited states in odd nuclei

Nuclear structure calculations have been performed within the QPM (see, e.g., Refs. [14,15,22–27]). This model has already been used in spectroscopic studies of odd nuclei over a wide mass region [14,15]. The application of the model in the case of isomeric states is described in detail in Refs. [6–9]. This model makes use of a separable form of the residual interaction which enables the diagonalization of the model Hamiltonian in a large dimensional configuration space.

The following wave function describes the ground and excited states of the odd nucleus with angular momentum J and projection M :

$$\Psi_{JM}^\vartheta = C_J^\vartheta \left\{ \alpha_{JM}^+ + \sum_{\lambda\mu i} D_j^{\lambda i}(J\vartheta) [\alpha_{jm}^+ Q_{\lambda\mu i}^+]_{JM} \right\} \Psi_0. \quad (11)$$

The notation α_{jm}^+ is the quasiparticle creation operator with shell quantum numbers $j \equiv (n, l, j)$ and m ; $Q_{\lambda\mu i}^+$ denotes the phonon creation operator with the angular momentum λ , projection μ and RPA root number i ; Ψ_0 is the ground state of the neighboring even-even nucleus and ϑ stands for the number within a sequence of states of given J^π . Coefficients C_J^ϑ and $D_j^{\lambda i}$ are the quasiparticle and ‘‘quasiparticle \otimes phonon’’ amplitudes for the ϑ state.

The coefficients of the wave function (11), as well as the energy of the excited states, are found by diagonalization of the model Hamiltonian within the approximation of the commutator linearization. The components $\alpha_{jm}^+ Q_{\lambda\mu i}^+$ of the wave function (11) may violate the Pauli principle. To solve this problem, the exact commutation relations between quasiparticle and phonon operators are used [14,15]. An efficient pro-

cedure for the approximate treatment of the Pauli principle corrections has been proposed in Ref. [31]. It is applied to the present calculations.

It should be noted that the wave function (11) describes in detail the distribution of the single-particle component while the distribution of the ‘‘quasiparticle \otimes phonon’’ components could be more affected by including ‘‘quasiparticle \otimes two-phonon’’ configurations [14,15]. As demonstrated below in actual calculation, the transitions between quasiparticle components of the decaying intermediate and final states are mainly responsible for the population of the isomeric and ground states in (γ, n) reaction. For this reason, the wave function in the form of Eq. (11) should be considered as a suitable one to describe the process.

Only the direct γ decays of the intermediate states of the residual nuclei into the ground and isomeric states have been accounted for in the present studies. The lowest excited states of semimagic even-even nuclear core of isotopes under consideration have an excitation energy from 1.4 to 1.7 MeV. This means that only a few ‘‘quasiparticle \otimes three-phonon’’ and a very limited number of ‘‘quasiparticle \otimes two-phonon’’ configurations are available up to an excitation energy of 5.4 MeV. Thus, a configuration space for the cascade decays is very small and the direct decays should play a predominant role.

The Woods-Saxon potential $U(r)$ is used for the mean-field part of the QPM Hamiltonian with parameters from Refs. [32,33]. The corresponding single-particle spectra can be found in Ref. [14]. The residual particle-hole interaction is taken of separable form in coordinate space with radial form factor as $f(r) = dU/dr$. The strength of the residual interaction is adjusted to reproduce in one-phonon approximation the experimental energies and transition probabilities [34] of the lowest collective levels in the neighboring even-even nucleus for each J^π . The phonon basis is obtained by solving the QRPA equations. The coupling matrix elements between quasiparticle and ‘‘quasiparticle \otimes phonon’’ configurations are calculated using the internal fermion structure of the phonons and the model Hamiltonian with all parameters fixed from the calculations in the even-even core.

In the calculations presented below we have used $\lambda^\pi = 1^\pm, 2^+, 3^-, 4^+, \text{ and } 5^-$ phonons in the wave function (11). Several roots for each multipolarity are taken into account. The maximum energy of ‘‘quasiparticle \otimes phonon’’ configurations included in Eq. (11) equals 12 MeV.

The used effective charges are: for $E1$ transitions $e_{\text{eff}}^p = (N/A)e$ and $e_{\text{eff}}^n = -(Z/A)e$ to separate a center of mass motion; ‘‘free’’ values for $E2$ transitions $e^n = 0$ and $e^p = 1$ because our single-particle basis is rather complete; and for $M1$ transitions the effective spin g^s factor is $g_{\text{eff}}^s = (0.8)g_{\text{free}}^s$. The last value often has been used in the past in QPM calculation of magnetic moments [29], low energy magnetic transitions [28], and excitation probability of $M1$ and $M2$ resonances [30] in medium and heavy nuclei. The reduction factor 0.8 provides the best agreement with experimental data available. The numerical calculations presented in this article have been performed with the code PHOQUS [31].

TABLE III. The calculated energies (QPM) of the isomeric state $h_{11/2}$ in ^{137}Ba , ^{139}Ce , ^{141}Nd , and ^{143}Sm in comparison with the experimental values (Exp) from Ref. [19]. The main components of the isomeric wave function are presented in the the last two columns.

	E , MeV		α^+	$\alpha^+ Q^+$
	Exp	QPM		
^{137}Ba	0.662	0.660	$1h_{11/2}(83.9\%)$	$1h_{11/2} \otimes 2_1^+(7.2\%) + 2d_{5/2} \otimes 3_1^-(1.5\%)$
^{139}Ce	0.754	0.725	$1h_{11/2}(84.9\%)$	$1h_{11/2} \otimes 2_1^+(8.1\%) + 2d_{5/2} \otimes 3_1^-(1.4\%)$
^{141}Nd	0.757	0.795	$1h_{11/2}(86.2\%)$	$1h_{11/2} \otimes 2_1^+(5.6\%) + 2d_{5/2} \otimes 3_1^-(1.9\%)$
^{143}Sm	0.754	0.786	$1h_{11/2}(84.6\%)$	$1h_{11/2} \otimes 2_1^+(6.2\%) + 2d_{5/2} \otimes 3_1^-(2.5\%)$

IV. THEORETICAL ANALYSIS OF THE EXPERIMENTAL DATA

The IR is studied along the isotopic chain $N=81$ including nuclei ^{137}Ba , ^{139}Ce , ^{141}Nd , and ^{143}Sm . First, the properties of the $(11/2^-)$ isomeric state are reproduced well in calculation. Its excitation energy is known to be approximately the same for all nuclei under consideration (see experimental data in second column of Table III). The calculated energy of the isomeric state (third column of Table III) is in agreement with the data. Its structure is dominated by the single-particle component, but the coupling with the quadrupole and octupole vibrations of the core is also important. The calculated structure of the isomeric state is also in agreement with the recent measurements [19].

In addition, the spectrum of the excited states has been calculated with $J^\pi = 1/2^\pm$, $3/2^\pm$, $5/2^\pm$, $7/2^\pm$, $9/2^+$, and $11/2^-$ up to the excitation energy of 6.5 MeV. The states with lower values of angular momentum are responsible for population of the ground state in (γ, n) reaction while among other states we are looking for the AS. The spectra of states with $J > 11/2$ have not been calculated because they cannot be populated in the neutron decay of the GDR. The corresponding partial widths $\Gamma_{J_i \rightarrow J_f}$ and the main components contributing in the structure of the excited states are given in Table IV for ^{139}Ce .

The population of the isomeric state $(11/2^-)$ in ^{139}Ce is mainly due to the $E1$ transitions from the $J^\pi = 9/2^+$ states. The distribution of the single-particle component $9/2^+$ of the wave function (11) up to 6.5 MeV is shown in Fig. 3(b). A visible fraction of $9/2^+$ single-particle component (14% of the whole strength) is spaced in this energy region. There are two excited states at 4.18 and 6.15 MeV, where 4.7 and 5.2% of the single-particle strength is concentrated. The main components in the structure of the excited states are due to the coupling of the single-particle mode with the surface vibrations of the even core. The dependence of the quantity $C^2\Gamma_{J^\pi \rightarrow \text{iso}}$ on the excitation energy is shown in Fig. 3(a). The contribution of the $E1$ transitions dominates, but also $E2$ transitions are important. The comparison of Fig. 3(a) and Fig. 3(b) reveals a bright correlation between the distribution of $C^2\Gamma_{9/2^+ \rightarrow \text{iso}}$ ($E1$) and those of the single-particle component $9/2^+$. The higher concentration of the single-particle component leads to larger $E1$ transitions into the isomeric state.

The $7/2^-$ states populate the isomeric state by $E2$ transitions. The distribution of the single-particle component $7/2^-$

of the wave function (11) is shown in Fig. 3(c). There are two main states at 3.22 and 4.88 MeV where 0.6 and 0.4% of the single-particle strength is concentrated. By comparing Fig. 3(a) and Fig. 3(c), it can be concluded that there is also a correlation between the distribution of the single-particle component $7/2^-$ and the quantity $C^2\Gamma_{7/2^- \rightarrow \text{iso}}(E2)$: large single-particle component in the wave function (11) leads to larger $E2$ transitions. Taking into account the foregoing properties of $E1$ and $E2$ transitions one concludes that the structure of the quantity $C^2\Gamma_{J^\pi \rightarrow \text{iso}}$ is completely determined by the contribution of the single-particle component in the wave function (11).

The energy dependence of the quantity $C^2\Gamma_{J^\pi \rightarrow \text{g.s.}}$ in ^{139}Ce and the contribution of $E1$, $E2$, and $M1$ transitions are shown in Fig. 4. These transitions are due to the deexcitation of $1/2^\pm$, $3/2^\pm$, $5/2^+$, and $7/2^+$ states. The large $E1$ transitions to the ground state are concentrated at higher excitation energies. A state with $J^\pi = 1/2^-$ at 5.35 MeV gives the main part of the $E1$ transitions to the ground state in ^{139}Ce . In the structure of the state, the single-particle component is 6%, while the $(2d_{5/2} \otimes 3_1^-)$ component contributes 61.2%.

The $M1$ transitions to the ground state are predominantly due to the deexcitation of the $5/2^+$ states. The excitation energy of the first $5/2^+$ state is 1.49 MeV. The single-particle component dominates in the structure (68%) and it determines the largest value of $C^2\Gamma(M1)$ in the domain up to 6.5 MeV.

The $E2$ transitions to the ground state arise from the deexcitation of the states $1/2^+$, $3/2^+$, $5/2^+$, and $7/2^+$. The state $1/2^+$ (2.93 MeV) has the largest income in the population of the ground state via $E2$ transition. The single-particle component in the structure of the state is 5.5%. The $E2$ transition from the latter to the ground state presents around 6.5% of the sum of $\sigma_{\text{g.s.}}$ in Eq. (9).

The distribution of the single-particle configuration over the states with $J^\pi = 1/2^-, 3/2^-, 5/2^+, 7/2^+$ in ^{139}Ce up to 6.5 MeV is shown in Figs. 4(b)–4(e). The comparison of Fig. 4(a) and Figs. 4(b)–4(e) reveals again a correlation between the quantity $C^2\Gamma_{J^\pi \rightarrow \text{g.s.}}$ and those of the single-particle strength. The energy dependence of $C^2\Gamma_{J^\pi \rightarrow \text{g.s.}}$ is strongly connected to the amplitude value of the single-particle component of the wave function (11). The structure of $1/2^+$ and $3/2^+$ states and the corresponding value of $\Gamma_{J^\pi \rightarrow \text{g.s.}}$ are given in Table IV. The population of the ground up to 4.8 MeV is by $E2$ and $M1$ transitions. Only a few

TABLE IV. Some selected excited states in ^{139}Ce obtained in QPM calculations in the energy range up to 6.5 MeV with the largest values of the partial widths $\Gamma_{J_i \rightarrow J_f}$ for the direct decay into the ground and isomeric states. The quasiparticle (α^+) and the main ‘‘quasiparticle \otimes phonon’’ (α^+Q^+) components to their wave function are given in the last two columns.

J_i	E , MeV	Tran. $\lambda\lambda$	J_f	$\Gamma_{J_i \rightarrow J_f}$, eV	α^+	α^+Q^+
$1/2^+$	2.93	$E2$	$3/2^+$ (g.s.)	0.046	$3s_{1/2}$ (5.5%)	$2d_{3/2} \otimes 2_1^+$ (91.4%)
$1/2^+$	4.40	$E2$	$3/2^+$ (g.s.)	0.259	$3s_{1/2}$ (0.4%)	$2d_{3/2} \otimes 2_4^+$ (90.9%)
$1/2^+$	4.80	$E2$	$3/2^+$ (g.s.)	0.017	$3s_{1/2}$ (3.8%)	$2d_{5/2} \otimes 2_1^+$ (79.8%)
$1/2^+$	5.13	$E2$	$3/2^+$ (g.s.)	0.008	$3s_{1/2}$ (1.3%)	$1g_{7/2} \otimes 4_1^+$ (93%)
$1/2^-$	5.35	$E1$	$3/2^+$ (g.s.)	2.420	$2p_{1/2}$ (6.0%)	$2d_{5/2} \otimes 3_1^-$ (61.2%)
$1/2^-$	5.64	$E1$	$3/2^+$ (g.s.)	0.142	$2p_{1/2}$ (0.3%)	$1g_{7/2} \otimes 3_1^-$ (63.9%)
$3/2^+$	2.82	$E2$	$3/2^+$ (g.s.)	0.045	$2d_{3/2}$ (1.2%)	$2d_{3/2} \otimes 2_1^+$ (86.1%)
$3/2^+$	3.08	$M1$	$3/2^+$ (g.s.)	0.002	$2d_{3/2}$ (3.7%)	$3s_{1/2} \otimes 2_1^+$ (84.4%)
$3/2^+$	4.40	$E2$	$3/2^+$ (g.s.)	0.270	$2d_{3/2}$ (0.3%)	$2d_{3/2} \otimes 2_4^+$ (96.2%)
$3/2^-$	3.46	$E1$	$3/2^+$ (g.s.)	0.013	$2p_{3/2}$ (1.1%)	$1h_{11/2} \otimes 4_1^+$ (93%)
$3/2^-$	5.09	$E1$	$3/2^+$ (g.s.)	0.056	$2p_{3/2}$ (1.5%)	$1h_{11/2} \otimes 4_4^+$ (95.4%)
$3/2^-$	5.53	$E1$	$3/2^+$ (g.s.)	0.030	$2p_{3/2}$ (0.7%)	$2d_{5/2} \otimes 3_1^-$ (84.5%)
$5/2^+$	1.49	$M1$	$3/2^+$ (g.s.)	0.009	$2p_{3/2}$ (68%)	$3s_{1/2} \otimes 2_1^+$ (8%)
$5/2^+$	2.78	$E2$	$3/2^+$ (g.s.)	0.049	$2d_{5/2}$ (0.7%)	$2d_{3/2} \otimes 2_1^+$ (93.2%)
$5/2^+$	3.21	$M1$	$3/2^+$ (g.s.)	0.008	$2d_{5/2}$ (5.3%)	$2d_{3/2} \otimes 4_1^+$ (57.1%)
$5/2^+$	4.32	$E2$	$3/2^+$ (g.s.)	0.047	$2d_{5/2}$ (2.2%)	$1h_{11/2} \otimes 3_1^-$ (62.4%)
$5/2^+$	4.4	$E2$	$3/2^+$ (g.s.)	0.226	$2d_{5/2}$ (0.8%)	$2d_{3/2} \otimes 2_4^+$ (78.6%)
$5/2^+$	4.9	$M1$	$3/2^+$ (g.s.)	0.016	$2d_{5/2}$ (2.9%)	$2d_{5/2} \otimes 4_1^+$ (44%)
$5/2^+$	5.01	$M1$	$3/2^+$ (g.s.)	0.011	$2d_{5/2}$ (2.4%)	$2d_{5/2} \otimes 4_1^+$ (41.8%)
$5/2^+$	5.13	$M1$	$3/2^+$ (g.s.)	0.028	$2d_{5/2}$ (2.5%)	$1g_{7/2} \otimes 4_1^+$ (33.7%)
$5/2^+$	6.29	$M1$	$3/2^+$ (g.s.)	0.018	$2d_{5/2}$ (1.3%)	$2d_{5/2} \otimes 2_4^+$ (78%)
$7/2^+$	2.02	$E2$	$3/2^+$ (g.s.)	0.006	$1g_{7/2}$ (59.9%)	$2d_{3/2} \otimes 2_1^+$ (28.8%)
$7/2^+$	2.98	$E2$	$3/2^+$ (g.s.)	0.03	$1g_{7/2}$ (10.6%)	$2d_{3/2} \otimes 2_1^+$ (55.6%)
$7/2^+$	3.17	$E2$	$3/2^+$ (g.s.)	0.005	$1g_{7/2}$ (6.7%)	$2d_{3/2} \otimes 4_1^+$ (68%)
$7/2^+$	3.38	$E2$	$3/2^+$ (g.s.)	0.002	$1g_{7/2}$ (6.4%)	$3s_{1/2} \otimes 4_1^+$ (71.5%)
$7/2^+$	4.43	$E2$	$3/2^+$ (g.s.)	0.271	$1g_{7/2}$ (1.4%)	$2d_{3/2} \otimes 2_4^+$ (90.6%)
$7/2^+$	4.85	$E2$	$3/2^+$ (g.s.)	0.008	$1g_{7/2}$ (3%)	$1g_{7/2} \otimes 2_1^+$ (56.1%)
$7/2^-$	3.22	$E2$	$11/2^-$ (iso)	0.045	$1f_{7/2}$ (0.6%)	$1h_{11/2} \otimes 2_1^+$ (98.5%)
$7/2^-$	4.88	$E2$	$11/2^-$ (iso)	0.232	$1f_{7/2}$ (0.4%)	$1h_{11/2} \otimes 2_4^+$ (98.8%)
$9/2^+$	4.18	$E1$	$11/2^-$ (iso)	0.793	$1g_{9/2}$ (4.7%)	$1h_{11/2} \otimes 3_1^-$ (86.3%)
$9/2^+$	4.62	$E1$	$11/2^-$ (iso)	0.417	$1g_{9/2}$ (1.7%)	$2d_{5/2} \otimes 2_1^+$ (84.9%)
$9/2^+$	5.03	$E1$	$11/2^-$ (iso)	0.188	$1g_{9/2}$ (0.6%)	$2d_{5/2} \otimes 4_1^+$ (52.3%)
$9/2^+$	6.15	$E1$	$11/2^-$ (iso)	3.07	$1g_{9/2}$ (5.2%)	$1h_{11/2} \otimes 3_3^-$ (58.4%)
$9/2^+$	6.30	$E1$	$11/2^-$ (iso)	0.326	$1g_{9/2}$ (0.5%)	$2d_{5/2} \otimes 2_4^+$ (61%)

states perceptibly influence the value of $C^2\Gamma_{J\pi \rightarrow \text{g.s.}}$.

The same type of calculation has been performed for the other isotones. They are not discussed here in detail because the results and conclusions are very similar to the ones already presented for ^{139}Ce . The conclusion for all isotones under consideration is that the population of the isomeric state as well as those for the ground state depends on the distribution of the single-particle component of the wave function (11) over the AS.

It follows from the presented figures that the IR defined in Eq. (9) depends strongly on the maximum excitation energy of the final nucleus. The number of excited states at intermediate energies involved in the process varies when the excitation energy is changed and the number of large $E1$, $E2$,

and $M1$ transitions populating isomeric and ground state is also changed. The available experimental information obtained in (γ, n) reaction on the IR for $N=81$ nuclei is given in Table I. It is completed by the IR in two heaviest isotones known from β decay data [19]. Thus, in the case of ^{141}Nd and ^{143}Sm , two values of the IR are known corresponding to different maximum excitation energies E^* . The calculated values of the IR of Eq. (9) are given in Table I for comparison. The truncation of the AS included in the calculation by maximum excitation energy is made in accordance with experimental conditions. The calculated values agree very well with the measured ones. The energy dependence of the IR in the case of ^{141}Nd and ^{143}Sm is reproduced. In the case of ^{143}Sm up to excitation energy 3.5 MeV there are two

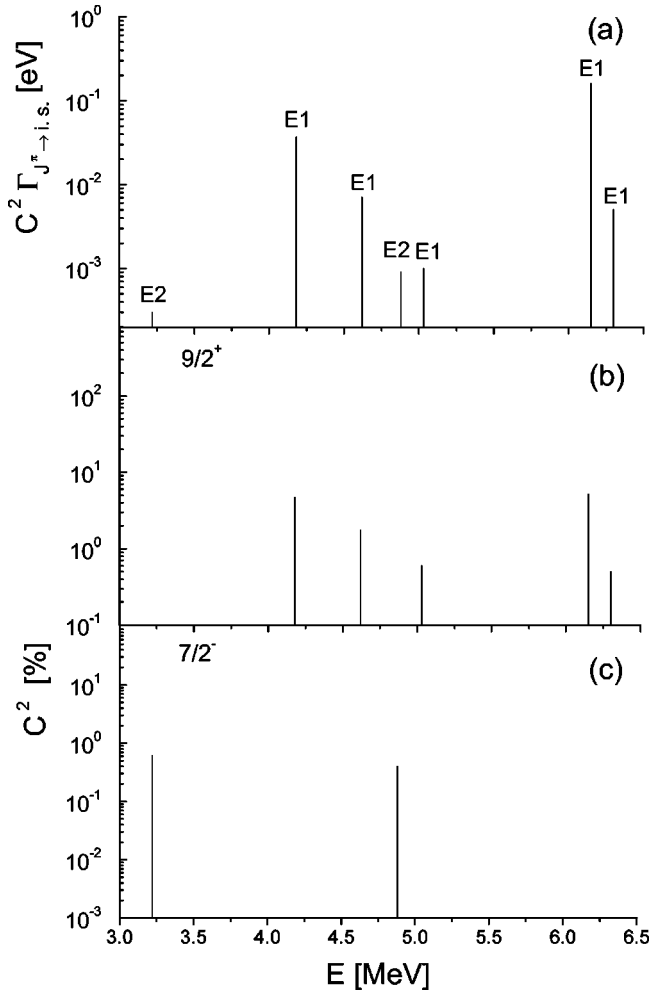


FIG. 3. (a) Decay probability $C^2 \Gamma$ for population of the isomeric state in ^{139}Ce from excited states at intermediate energies; (b),(c) contribution of one-quasiparticle configuration C^2 to wave functions of decaying states with different spin and parity. The multipolarity of each transition is indicated on top of lines in (a). J^π of decaying states is specified in (b) and (c).

states— $9/2^+$ at 3.48 MeV and $7/2^-$ at 3.46 MeV. These states are connected with the isomer by $E1$ and $E2$ transitions. The increase of the excitation energy up to 4.72 MeV does not influence the value of $C^2 \Gamma_{J^\pi \rightarrow iso}$ while the value of $C^2 \Gamma_{J^\pi \rightarrow g.s.}$ is changed due to the $E2$ and $M1$ transitions connected the $1/2^+$, $5/2^+$, and $7/2^+$ states with the ground state. The situation is similar in ^{141}Nd .

V. CONCLUSIONS

The IR in $N=81$ and $Z=56-62$ nuclei obtained in (γ, n) reaction on the beam of bremsstrahlung were measured. The

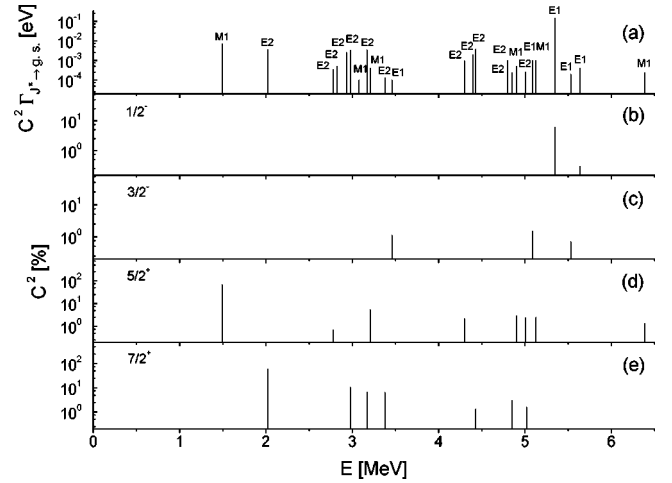


FIG. 4. The same as in Fig. 3 for population of the ground state in ^{139}Ce .

large difference of the IR for the studied nuclei was observed in spite of the similar properties of the isomeric states. The measured values are completed by available experimental information obtained from β^- decay. The new set of data reveals a dependence of the IR on a maximum excitation energy of residual nuclei reached in (γ, n) reaction and β^- decay.

The calculation of the IR in the framework of QPM is done. It is shown that the value of the IR depends on the contribution of the corresponding single-particle component in the structure of the wave function of the excited state. The IR as a function of the excitation energy of a residual nucleus is determined by the fluctuation in the distribution of the single-particle components. The maximum energy of the intermediate states populated in (γ, n) reaction is responsible for the truncation of the states involved in the forthcoming decay to the ground and isomeric states. That is why the IR in ^{137}Ba and ^{139}Ce with somewhat higher values of the maximum excitation energy is different from the ones in ^{141}Nd and ^{143}Sm . Our calculation reproduces rather well the IR dependence on A as well as the absolute values of the IR in all isotones under consideration.

ACKNOWLEDGMENTS

The present work is partly supported by the Bulgarian Science Foundation (Contract No. Ph. 626) and Plovdiv University (Contract No. PU F-23). V. Yu. P. acknowledges support from the Research Council of the University of Gent and NATO. Finally, we would like to thank Lynn Leonard for her careful reading of this paper.

- [1] Yu. P. Gangrsky, A. P. Tonchev, and N. P. Balabanov, *Fiz. Elem. Chastits At. Yadra* **27**, 1043 (1996).
 [2] A. G. Belov, Yu. P. Gangrsky, A. P. Tonchev, and N. P. Balabanov, *Yad. Fiz.* **59**, 585 (1996).
 [3] V. M. Mazur, V. A. Jeltonojksij, and Z. M. Bigan, *Yad. Fiz.*

58, 970 (1995).

- [4] V. M. Mazur, Z. M. Bigan, and I. V. Sokolyuk, *Laser Phys.* **5**, 273 (1995); V. M. Mazur, I. V. Sokolyuk, and Z. M. Bigan, *Yad. Fiz.* **54**, 895 (1991).
 [5] A. P. Dubenskiy, V. P. Dubenskiy, A. A. Bojkova, and L.

- Malov, Bull. Acad. Sci. USSR, Phys. Ser. **57**, 90 (1993).
- [6] V. Ponomarev, A. P. Dubenskiy, V. P. Dubenskiy, and E. A. Boykova, J. Phys. G **16**, 1727 (1990).
- [7] P. von Neumann-Cosel, V. Yu. Ponomarev, A. Richter, and C. Spieler, Z. Phys. A **350**, 303 (1995).
- [8] J. J. Carrol, C. B. Collins, K. Heyde, M. Huber, P. von Neumann-Cosel, V. Yu. Ponomarev, D. G. Richmond, A. Richter, C. Schlegel, T. W. Sinor, and K. N. Taylor, Phys. Rev. C **48**, 2238 (1993).
- [9] M. Huber, P. von Neumann-Cosel, A. Richter, C. Schlegel, R. Schulz, J.J. Carroll, K. N. Taylor, D. G. Richmond, T. W. Sinor, C. B. Collins, and V. Yu. Ponomarev, Nucl. Phys. **A559**, 253 (1993).
- [10] A. P. Tonchev, Yu. P. Gangrsky, A. G. Belov, and V. E. Zhuchko, Phys. Rev. C **58**, 2851 (1998).
- [11] L. Ya. Arifov, B. S. Mazitov, and V. G. Ulanov, Yad. Fiz. **34**, 1028 (1981).
- [12] R. Vandenbosch and J. R. Huizenga, Phys. Rev. **120**, 1305 (1960); **120**, 1313 (1960).
- [13] A. V. Ignatjuk, G. N. Smirenkin, and A. S. Tishin, Yad. Fiz. **21**, 485 (1975).
- [14] S. Gales, Ch. Stoyanov, and A. I. Vdovin, Phys. Rep. **166**, 125 (1988).
- [15] A. I. Vdovin, V. V. Voronov, V. G. Soloviev, and Ch. Stoyanov, Part. Nuclei **16**, 245 (1985).
- [16] V. Yu. Ponomarev, V. G. Soloviev, Ch. Stoyanov, and A. I. Vdovin, Phys. Lett. B **183**, 237 (1987).
- [17] Nguen Van Giai, Ch. Stoyanov, V. V. Voronov, and S. Fortier, Phys. Rev. C **53**, 730 (1996).
- [18] B. L. Berman, S. C. Fultz, J. T. Caldwell, M. A. Kelly, and S. S. Dietrich, Phys. Rev. C **2**, 2318 (1970).
- [19] T. W. Burrows, Nucl. Data Sheets **57**, 399 (1989); J. K. Tuli, *ibid.* **72**, 369 (1994); **45**, 106 (1985); **48**, 812 (1986).
- [20] A. Bohr and B. Mottelson, in *Single-Particle Motion*, Vol. 1 of *Nuclear Structure* (Nordita, Copenhagen, 1969).
- [21] G. I. Marchuk and V. E. Kolesov, *Application of Numerical Methods for Calculation of Neutron Cross Sections* (Atomizdat, Moskva, 1970).
- [22] V. G. Soloviev, *Theory of Complex Nuclei* (Pergamon Press, Oxford, 1976).
- [23] V. G. Soloviev, *Theory of Atomic Nuclei: Quasiparticles and Phonons* (Institute of Physics Publishing, Bristol, 1992).
- [24] V. G. Soloviev, Ch. Stoyanov, and A. I. Vdovin, Nucl. Phys. **A342**, 261 (1980).
- [25] A. I. Vdovin and V. G. Soloviev, Part. Nuclei **14**, 237 (1983).
- [26] V. V. Voronov and V. G. Soloviev, Part. Nuclei **14**, 1380 (1983).
- [27] C.A. Bertulani and V.Yu. Ponomarev, Phys. Rep. **321**, 139 (1999).
- [28] T.K. Dinh, M. Grinberg, and Ch. Stoyanov, J. Phys. G **18**, 329 (1992); M. Grinberg, Ch. Stoyanov, and N. Tsoneva, Fiz. Elem. Chastits At Yadra **29**, 1456 (1998).
- [29] A.I. Vdovin, R.R. Safarov, and V.Yu. Ponomarev, Bull. Acad. Sci. USSR, Phys. Ser. **54(9)**, 149 (1990).
- [30] V.Yu. Ponomarev, V.G. Soloviev, Ch. Stoyanov, and A.I. Vdovin, Nucl. Phys. **A323**, 446 (1979); A.I. Vdovin, V.V. Voronov, V.Yu. Ponomarev, and Ch. Stoyanov, Sov. J. Nucl. Phys. **30**, 479 (1979).
- [31] Ch. Stoyanov and C. Q. Khuong, JINR Dubna Report No. P-4-81-234, 1981 (unpublished).
- [32] V. A. Chepurnov, Sov. J. Nucl. Phys. **6**, 955 (1967).
- [33] K. Takeuchi and P. A. Moldauer, Phys. Lett. **28B**, 384 (1969).
- [34] P. M. Endt, At. Data Nucl. Data Tables **42**, 1 (1989); S. Raman, W. C. Nestor, Jr., S. Kahane, and K.H. Bhatt, *ibid.* **42**, 1 (1989).